A piglet model of iatrogenic rectosigmoid hypoganglionosis reveals the impact of the enteric nervous system on gut barrier function and microbiota postnatal development

Alexis Pierre Arnaud, Juliette Hascoet, Pauline Berneau, Francis Legouevec, Julien Georges, Gwenaëlle Randuineau, Michele Formal, Sébastien Henno, Gaëlle Boudry

HAL Id: hal-02911607
https://hal.inrae.fr/hal-02911607v1

Submitted on 25 Aug 2020

A piglet model of iatrogenic recto-sigmoïd hypoganglionosis reveals the impact of the enteric nervous system on gut barrier function and microbiota post-natal development

Alexis Pierre Arnaud[a, b]*, Juliette Hascoet[a] , Pauline Berneau[a], Francis LeGouevec[c], Julien Georges[c], Gwenaelle Randuineau[a], Michèle Formal[a], Sébastien Henno[d], Gaelle Boudry[a]

[a] Institut NuMeCan INRAE, INSERM, Univ Rennes, Saint-Gilles, France.

[b] Service de chirurgie pédiatrique, CHU Rennes, Univ Rennes, Rennes, France

[c] UEPR, INRA, Saint-Gilles, France.

[d] Service d'anatomo-pathologie, CHU Rennes, Univ Rennes, Rennes, France

* Corresponding author

Dr Alexis P ARNAUD, MD, PhD

Service de chirurgie pédiatrique

Hopital Sud, CHU Rennes

16 boulevard de Bulgarie

35203 Rennes cedex2

France

E-mail : Alexis.Arnaud@chu-rennes.fr

Phone number : 0033 681691670

Abstract

Background: Hirschsprung-associated enterocolitis physiopathology likely involves disturbed interactions between gut microbes and the host during the early neonatal period. Our objective was to create a neonatal porcine model of iatrogenic aganglionosis to evaluate the impact of the enteric nervous system (ENS) on microbiota and intestinal barrier post-natal development. **Methods:** Under general anesthesia, the recto-sigmoid serosa of 5-day old suckling piglets was exposed to 0.5% benzalkonium chloride solution (BAC, n=7) or saline (SHAM, n=5) for 1hr. After surgery, animals returned to their home-cage with the sow and littermates and were studied 21 days later. **Results:** BAC treatment induced partial aganglionosis with absence of myenteric plexus and reduced surface area of sub-mucosal plexus ganglia (-58%, P<0.05) in one third of the recto-sigmoid circumference. Epithelial permeability of this zone was increased (conductance +63%, FITC-dextran flux +386%, horseradish-peroxidase flux +563%, P<0.05). Tight junction protein remodeling was observed with decreased ZO-1 (-95%, P<0.05) and increased claudin-3 and e-cadherin expressions (+197% and 61%, P<0.05 and P=0.06, respectively). BAC piglets harbored greater abundance of pro-inflammatory bacteria (*Bilophila, Fusobacterium*) compared to SHAM in the recto-sigmoid lumen. **Conclusions:** This large animal model demonstrates that hypoganglionosis is associated with dramatic defects of gut barrier function and establishment of pro-inflammatory bacteria.

ABBREVIATIONS: AJ: adherens junction, BAC: benzalkonium chloride solution, ENS: enteric nervous system, FD-4: FITC-dextran 4000, G: conductance, HAEC: Hirschspung-disease associated enterocolitis, HD: Hirschsprung disease, HRP: horseradish peroxidase, PBS: phosphate buffer saline, PGP: protein gene product, TBS-T: Tris buffer saline-Tween, TJ: tight junction, VIP: vasoactive intestinal peptide

1. Introduction

Hirschsprung disease (HD) is a congenital disorder of the intestinal tract characterized by the absence of ganglionic cells (aganglionosis) in myenteric and sub-mucosal plexi of the distal gut resulting from the failure of the neural crest cells migration [1,2]. This defect of the enteric nervous system (ENS) is responsible of neonatal bowel obstruction that requires surgical care and resection of the aganglionic segment. The most serious and life-threatening complication of HD is the development of Hirschsprung associated enterocolitis (HAEC). HAEC is a severe inflammatory colitis that causes distension, diarrhea, fever, and can lead to bacterial translocation, sepsis and death. Its pathogenesis remains unclear although many hypotheses have been proposed such as modifications of intestinal barrier function, innate immunity or microbiota composition [3,4]. Indeed, gut microbiota and intestinal barrier co-develop after birth, establishing a homeostatic state whereby mucosal cells cohabit with commensal bacteria. Altered neonatal colonization and disturbed interactions between gut microbes and the host during the neonatal period have profound effects on health [5]. The ENS is involved in all gut functions. Its role on intestinal barrier function was revealed by the use of tetrodotoxin that blocks nervous influx, with contrasting effects depending on the species used [6–9]. A role of the ENS on microbiota composition is also suspected since dysbiosis has been described in animal models of aganglionosis [10]. Despite these described effects of the ENS on adult gut barrier function and microbiota, the role of ENS on the post-natal development of microbiota-host interaction is still poorly described but would constitute a step forward in the understanding of HAEC.

Most of the studies on the role of ENS on microbiota and barrier function were performed in rodent adult models. However, intestinal post-natal development in rodents is different from Humans since these species are born with extremely immature intestine. The piglet model is known for its proximity with Humans in terms of intestinal physiology and foetal and neonatal development [11]. The relevance of using the pigs as an experimental model has previously been described: best non primate model for studying human nutrition [12] and tolerance to

4

food antigens (large single stomached omnivore) [13], model for a variety of human disease risk factors (obesity, stress, diabetes) and drug metabolism [14], realistic model of the human gastrointestinal tract to study microbiota [15]. Intestinal homeostasis factors that could be involved in the pathogenesis of HAEC, such as permeability and microbiota composition have been described in both species. The pig gut is closer to Human than rodents in terms of para and trans cellular permeability with a similar regulation [16]. Regarding the microbiota, Human and pigs have a high rate of Firmicutes and Bacteroidetes [11], and their fecal and colic microbiota present with a higher similarity than with other species[12,17–19]. However, contrary to rodent models, no genetic model of intestinal aganglionosis are available to study the role of ENS on microbiota and intestinal barrier post-natal development. In 1978, Sato et al produced segmental aganglionosis by applying benzalkonium chloride solution (BAC) to the outer surface of the recto-sigmoid in adult rats [20]. BAC is a detergent with tension-active properties inducing membrane cell depolarization leading to cell death. The specific effect of BAC application on ganglionic cells remains unclear and could rely on higher negative charge of these cells or a specific immune system activation [21,22]. This model has been used to study the impact of aganglionosis on various intestinal segments of adult mice and rats [22–26] as well as to test pharmacological strategies for enteric neurons recovery after damage [27–29].

In the present study, we used a similar approach in neonatal piglets to evaluate the functional consequences of aganglionosis on epithelial barrier function and microbiota during the neonatal period in a model close to Humans.

2. Materials and methods

2.1. Animal and study design

This study was carried out in strict accordance with the recommendations for the care and use of animals for experiments. The protocol was approved by the Ethical Committee on animal experiments of Rennes (Approval number 2015080515242437). The experiments complied with the French law on animal experiments.

Twelve Largewhite x Landrace crossbred suckling piglets from 3 different litters and with an average birth weight of 1.83 ± 0.34 kg were included. Piglets were housed in the farrowing crate (2.7 x 1.8 m, partly slatted floor and stall length 2.0 m with adjustable width) with the sow and their littermates (12 to 14 piglets per litter in total, including 2-3 BAC piglets and 1-2 SHAM piglets per litter). Artificial lighting was provided between 0800 and 1800 h, and the ambient temperature was maintained between 22 and 25°C. In each farrowing crate, an infrared lamp provided an additional heat source for the piglets. No creep-feeding was offered during the whole period and piglets had theoretically no access to sow's feed. Surgery was performed at 5 days of age. Animals were fasted 1 hour before surgery. Anesthesia was induced and maintained with isoflurane (5% at induction then 1.6% for maintenance) in oxygen 30% after tracheal intubation. An ear vein was catheterized and animals were sedated with intravenous morphine (0.1mg/kg). The lungs were mechanically ventilated with volume-controlled ventilation (volume=8ml/kg, frequency=35/min). Body temperature was maintained between 38°C and 39°C with the use of an electric heated mat. Throughout surgery, saline solution was administered through the ear vein catheter (4 mL/kg/h). A sub-umbilical midline laparotomy was performed and the recto-sigmoid was isolated in a plastic drape. A 4-cm segment of recto-sigmoid was marked by serosal non absorbable suture tag and wrapped in gauze soaked with 0.5% BAC (Sigma Aldrich) as described by Pan et al in adult rats [27]. BAC solution was added continuously on the gauze in order to expose the recto-sigmoid serosal surface for one hour (BAC group). Then, the gauze was removed and the treated segment was rinsed with 10 mL of 0.9% saline. The same method with 0.9% saline instead of BAC was used for the sham piglets (SHAM group). The laparotomy was closed with continuous absorbable sutures in 2 layers. After recovery, piglets were brought back to the sow and their littermates. Suckling was thus possible one hour after the end of surgery. Animal were weighed twice a week. Painful behavior was checked and paracetamol was given if needed (15mg/kg, four times a day maximum). None of the piglets encountered health problem or bowel obstruction symptoms. Piglet growth was similar between the two groups. None of the piglets received antibiotics pre or post

6

procedure. Preliminary experiments were performed with 1% BAC (n=2 piglets) but this greater dose did not give better results on the intensity of the aganglionosis.

Animals were sacrificed by T61 intra-cardiac administration 21 days after surgery, i.e. at the age of 26 days. At sacrifice, the region of recto-sigmoid exposed to treatment was sampled, always in the same proximo-distal order. Samples were treated for histology, immunohistochemistry (ENS and tight junction (TJ) proteins), Western Blot and intestinal permeability measurement in Ussing chamber as described in the corresponding sections. Luminal contents in the recto-sigmoid treated region were sampled and immediately frozen for later microbiota analysis. Preliminary experiments were also performed with piglets sacrificed 7 days after BAC application to evaluate aganglionosis by immunohistochemistry and intestinal permeability with Ussing chambers (n=5/group).

2.2. Immunohistochemistry

Tissue specimens were immediately fixed in 4% paraformaldehyde and subsequently embedded in paraffin blocks. Blocks were cut into transversal 5 µm thick sections and mounted on adhesive slides. Tissues were de-waxed by immersion in xylene, rehydrated in alcohol and washed in distilled water. Slides were incubated in a solution of phosphate buffered saline (PBS) with 10% methanol and 3% H_2O_2 for one hour at room temperature for antigen retrieval. Non-specific sites were then blocked by immersing the slides in a 2% bovine serum albumin-PBS solution for one hour at room temperature. Slides were then incubated overnight at 4°C in a humidified slides chamber in primary antibodies against protein gene product 9.5, a neuronal marker (PGP 9.5; 1:1000, Cedarlane, Burlington, Ontario, Canada). After washing three times 10 min in PBS, slides were incubated in secondary antibodies anti rabbit FITC (1:200; Jackson ImmunoResearch, USA) for 2 hours at room temperature. Slides were then washed three times for 10 min in PBS. Finally, DAPI nuclear staining (Fluoroshield Mounitg Medium with DAPI) was performed and each section was covered with glass cover slips.

Sections were visualized under fluorescence microscopy (Nikon Eclipse 80i) and analyzed with NIS-Element D version 4.30 and image J softwares. The length of the aganglionic section of the myenteric plexus was measured and expressed as percentage of the total circumference. We could not clearly distinguish the inner sub-mucosal plexus and evaluated the impact of BAC treatment on the outer sub-mucosal plexus. For each plexus, the number and individual surface area of the ganglia were measured on the whole circumference. An average ganglia surface area and a total ganglia surface were calculated.

The same protocol was used for the staining of ZO-1 (220kDa, 1:125, Zymed), Claudin 3 (22KDa, 1:250, Invitrogen, USA) and E-cadherin (120kDa, 1:100, Dako) and Alexa Fluor F488 or F546 couples secondary antibodies (1:400, Life Technologies).

2.3. Histology

Histology blocks were cut into transversal 5 µm thick sections and mounted on adhesive slides. The tissues were de-waxed by immersion in xylene, rehydrated in alcohol and washed in distilled water. Sections were stained with haematoxylin-eosin, examined under a light microscope (Nikon Eclipse 80i) and analyzed with Image-J software.

Morphometric analysis included crypt depth and thickness of the longitudinal and circular smooth muscle layers. In the BAC group, only the musculosa and the mucosa facing the hypoganglionotic myenteric plexus section was analyzed. In the SHAM group, only the ante-mesenteric sections were analyzed. Ten to fifteen measures were carried out at regular intervals and averaged to get a representative value for each piglet.

2.4. Western blot

Freshly dissected recto-sigmoid tissue (ante-mesenteric section, corresponding to the hypo-ganglionic region in the BAC group) was instantly frozen in liquid nitrogen and stored at -80°C. A mechanical lysis was performed on 50 mg of tissue in 1 mL of RIPA lysis buffer (Sigma-Aldrich) plus protease inhibitors (Roche) with a Precellys® 24 (Bertin technologies). The homogenate was centrifuged at 14000 rpm for 15 min at 4°C. Protein concentration in

the supernatant was determined using a Lowry assay kit (Thermofisher). 10 µg of proteins were loaded on a NuPAGE 4-12%, Bis-tris Gel (Novex, Life Technologies) and run for 2 hours at 110 volts. Following electrophoresis, proteins were transferred to polyvinylidene difluoride membranes. Then, membranes were blocked with 5% blotting-grade blocker (Bio-Rad) in 0.1% Tris buffered saline tween solution (TBS-T) for one hour. Subsequently membranes were cut in 4 pieces according to the molecular weight scale and the corresponding membrane were incubated overnight at 4°C with agitation with primary antibodies against Claudin 3 (22KDa, 1:500, Invitrogen), E-cadherin (120kDa, 1:500, Dako), ZO-1 (220kDa, 1:1000, Zymed) and Actin (43 KDa, 1:1000, Sigma- Aldrich). Membranes were washed three times in TBS-T for 10 min and incubated with the horseradish peroxidase conjugated goat anti-rabbit IgG secondary antibody (1:10000, Sigma Aldrich) or horseradish peroxidase conjugated rabbit anti-mouse IgG secondary antibody (1:5000, Dako) for one hour at room temperature. After a final wash, signals were detected using a chemiluminescence system (ECL western blotting substrate, Lifetechnologies). Finally, membranes were scanned and analyzed with Quant TL software (GE Health care lifescience).

2.5. Measurement of intestinal permeability in Ussing chambers

Immediately after dissection, segments of recto-sigmoid were sampled and the ante-mesenteric region (corresponding to the hypoganglionic region in the BAC group) was mounted in Ussing chamber (Physiologic instruments, San Diego, CA) exposing 0.5 cm^2 of tissue area to 2.5 mL circulating oxygenated Krebs solution maintained at 39°C. Conductance (G) and FITC-4000 (FD4, Sigma Aldrich) and horseradish peroxidase (HRP, Sigma Aldrich) fluxes were measured as already described [30].

2.6. Microbiota analysis

Recto-sigmoid luminal contents were kept at -80°C until processing for DNA extraction using the ZR fecal DNA Miniprep (Ozyme). The V3-V4 region of DNA coding for 16SrRNA was

9

amplified using the following primer: CTTTCCCTACACGACGCTCTTCCGATCT ACTCCTACGGGAGGCAGCAG (V3F) and GGAGTTCAGACGTGTGCTCTTCCGATCT TACCAGGGTATCTAATCC (V4R), Taq Phusion (New England Biolabs) and dNTP (New England Biolabs) during 25 cycles (10 s at 98°C, 30s at 45°C, 45s at 72°C). Purity of amplicons was checked on agarose gels before sequencing using Illumina Miseq technology, performed at the Genotoul Get-Plage facility (Toulouse, France). The 16S rDNA raw sequences were analyzed using the bioinformatic pipeline FROGS [31] and the Phyloseq R package as well as LDA effect size (LEfSe) analysis [32], as already described [30].

2.7.   Statistical analysis

Quantitative variables are presented as mean and standard deviation of the mean. Statistical analysis was performed with Prism software (GraphPad Software, Inc) using Kruskal-Wallis tests. A probability value of $p<0.05$ was used as a cut-off for statistical significance.

3. Results

3.1.   Aganglionosis

PGP9.5 immunostaining revealed a loss of neurons and glial cells in the myenteric plexus with hypoganglionosis on the anti-mesenteric border of the treated recto-sigmoid (Figure 1). Denervated myenteric plexus represented $27 \pm 13\%$ of total recto-sigmoid circumference. This was confirmed by counting the number of ganglia over the whole circumference. BAC treatment induced a reduction of the number of ganglia in the myenteric plexus (-34%, p=0.005, Figure 2A). The average surface area of individual ganglia tended to be lower (-45%, P=0.059, Figure 2B). Total ganglia surface area was dramatically decreased by 62% in BAC compared to SHAM animals (p=0.002, Figure 2C).

The submucosal plexus was less altered by BAC treatment since submucosal ganglia were still observed on the total recto-sigmoid circumference. Yet, BAC induced a reduction of the number of ganglia in the outer submucosal plexus (-33%, p=0.005, Figure 2D). The average

surface area of individual ganglia was not altered by BAC treatment (Figure 2E). Total ganglia surface area was decreased by 58% in BAC compared to SHAM piglets (p=0.01, Figure 2F). Preliminary experiments with piglets sacrificed 7 days after BAC application showed relatively similar results for the myenteric plexus (denervation on 34 ± 9% of total recto-sigmoid circumference, reduction of 36% of the number of ganglia compared to SHAM piglets (p=0.02), no difference in the average surface of individual ganglia or total ganglia surface). However, the sub-mucosal plexus was not altered at that stage.

3.2. Morphology of the mucosa and muscle layers

Morphology of the mucosa and muscle layer was evaluated on the ante-mesenteric side of the recto-sigmoid, corresponding to the hypoganglionic zone. BAC treatment decreased external and internal muscle layers thickness (-57%, p=0.0002 and -38%, p< 0.0001, respectively, Figure 3 A&B). The muscle layer structures were macroscopically maintained. BAC treatment did not impact crypt depth (Figure 3C). Overall, the treated bowel was macroscopically similar to the sham one, without any perforation or inflammatory aspect.

3.3. Intestinal permeability

Likewise, we evaluated intestinal permeability on the ante-mesenteric side of the recto-sigmoid, corresponding to the hypoganglionotic zone. BAC treatment had no significant impact on short-circuit current (Isc) (Figure 4A). Conductance tended to be increased by BAC treatment (+63%, p=0.07, Figure 4B). BAC treatment induced a significant increase in HRP flux across the recto-sigmoid mucosa (+563%, p=0.006, Figure 4C). Similarly, paracellular permeability assessed by FD4 flux across the tissue was significantly greater in the BAC than in the SHAM group (+386%, p = 0.04, Figure 4D). In preliminary experiments with piglets sacrificed 7 days after BAC treatment, no difference in permeability was observed, irrespective of the parameter studied (data not shown).

3.4. Tight junction protein expression

11

Tight junction protein expression was evaluated on the ante-mesenteric side of the recto-sigmoid, corresponding to the hypoganglionotic zone. BAC treatment induced a profound remodeling of TJ protein expression with decreased expression of ZO-1 (-95%, p=0.035, Figure 5A and B) and increased expression of claudin 3 (+197%, p=0.01, Figure 5E and F) and a tendency for increased expression of e-cadherin (+61%, p=0.056, Figure 5I and J). These results were confirmed by immunohistochemistry performed on two parts of the recto-sigmoid of BAC piglets (healthy area on the mesenteric side and hypoganglionotic area on the ante-mesenteric side). Decreased ZO-1 immuno-staining on the hypoganglionotic section compared to the healthy section was observed (Figure 5 C&D). On the contrary, increased claudin3 and e-cadherin immuno-staining were observed in the hypoganglionotic section compared to the healthy section (Figure 5 G, H, K&L).

3.5. Luminal microbiota composition in piglets

BAC and SHAM recto-sigmoid luminal microbiota composition was assessed by 16SrDNA sequencing in 6 and 4 animals, respectively. BAC and SHAM microbiota clustered according to the treatment (Bray-Curtis index), with a large variability in the BAC group compared to the SHAM one (Figure 6A). Richness (Chao1 index) and diversity (Shannon index) were similar between groups (Figure 6B). At the phylum level, no clear changes appeared (Figure 6C), except for a tendency for increased Proteobacteria abundance in the BAC group compared to the SHAM one (9.2% [3.8-23.3] vs 2.9% [2.2-4.8], Mann Whitney test P=0.067). LDA effect size analysis revealed that the microbiota of BAC piglets was characterized by greater levels of *Fusobacterium* (Fusobacteria), *Mogibacterium* (Firmicutes) and *Bilophila* (Proteobacteria) while that of SHAM piglets was characterized by greater levels of *Solobacterium* (Firmicutes), *Shuttelworthia* (Firmicutes) and bacteria of the Lachnospiraceae family (Firmicutes) (Figure 6D).

4. Discussion

In the present study our objective was to create a model of iatrogenic aganglionnosis in a large animal model during the neonatal period to evaluate the impact of ENS on microbiota and intestinal barrier development. BAC application induced an hypoganglionnosis with absence of the myenteric plexus and reduced surface area of ganglia of the sub-mucosal plexus only in one third of the recto-sigmoid circumference. Yet, we were able to evaluate the consequences of this hypoganglionnosis with increased epithelial permeability and a profound remodeling of the tight junction proteins expression in the mucosa facing the hypo-ganglionnotic section. Luminal microbiota was also altered in this section.

Ideal animal models should be reproducible, cost-effective and accurately represent human physiology and anatomy of the disease to make results plausible [33]. Animal models of aganglionnosis have been previously reported [20–27,34–39], all involving small animals such as mice and rats, whose intestinal physiology and development are different from Human. The pig model is recognized as model of choice in terms of intestinal physiology and neonatal development [11,15,40]. The aganglionnosis was not complete all around the recto-sigmoid circumference. Presence of ganglia was always noted at the level of the mesentery attachment while total aganglionnosis was observed only in the myenteric plexus on the ante-mesenteric side. This was also the case in preliminary experiments where piglets were sacrificed 7 days after BAC application, suggesting that it was not a problem in the timing of the experiment (i.e. piglets studied too late after treatment). In pigs, the recto-sigmoid is firmly attached to the abdominal wall by a short, thick mesentery, as opposed to Humans where the mesocolon gives a relative mobility to the recto-sigmoid. Therefore, exposure of the entire serosal surface to BAC was not possible, probably explaining the partial aganglionnosis, located on the ante-mesenteric side of the recto-sigmoid, i.e. where the mesentery is thin. Yet, closer examinations of the number and size of ganglia revealed that the sub-mucosal plexus on the ante-mesenteric side was also affected by BAC treatment

13

with no effect on the average ganglia size but a lower number of ganglia in BAC animals, resulting in a lower total surface area of ganglia. This less efficient effect of BAC on the sub-mucosal plexus has been described previously in murine models [21,22,24,34,35]. Fox et al hypothesized that the detergent had difficulties to pass the internal muscle layer [34] but the literature is scarce on this topic. To note, the submucosal plexus was not altered at an earlier time point after BAC application, suggesting that the effect of BAC is not immediate. Finally, literature describes a concentration-dependent effect on denervation efficiency with a cut-off at 0.1% in mice [23,27,34]. Our preliminary experiment with 1% BAC did not give better results in terms of intensity of aganglionnosis and we kept the 0.5% BAC concentration to avoid any unspecific effect.

Both paracellular and transcellular permeabilities were dramatically increased in the epithelium of the hypoganglionnotic area. The enhanced recto-sigmoid permeability in BAC compared to SHAM piglets suggests that the ENS induces an inhibitory tonus on epithelial barrier function in SHAM animals. Intestinal epithelial permeability is controlled by the submucosal plexus [6,7]. Thus the reduced number of ganglia and total ganglia surface in the submucosal plexus of BAC treated piglets is probably at the origin of these differences in permeability. The fact that in our preliminary experiments with sacrifice 7 days after BAC treatment, no effect of BAC on the submucosal plexus was noticed and epithelial permeability was normal in BAC piglets strengthen this hypothesis. In piglet jejunum, nitriergic neurons are dominant at birth in the sub-mucosal plexus and decrease with age [41] while the density of VIPergic neurons increases progressively until 8 weeks of age [42–44]. Using VIP receptor agonist in Ussing chambers, our group demonstrated a VIPergic tonus on jejunal permeability at day 28 of age in piglets [45]. VIP has been shown to reduce paracellular epithelial permeability in *in vitro* cellular models or in adult rat intestine through the stimulation of ZO-1 expression [6,46–48]. VIP also reduces epithelial macromolecule transport by activation of the adenylate cyclase / AMPc pathway in rats [49]. No data on the chemical phenotype of the sub-mucosal plexus in the recto-sigmoid of neonatal piglets are

available but a VIPergic tonus in SHAM animals that was reduced in BAC piglets due to the overall decrease in ganglia number is plausible. The reduced expression of ZO-1 in the hypoganglionnotic section of the mucosa further strengthen this hypothesis. Such hypothesis is also consistent with the reduced VIP receptor density observed in Hirschsprung's disease patients [50] .

Tight junction proteins play a key role in the regulation of epithelial barrier function. Quantity, localization and phosphorylation state of these proteins along the intestine are under the control of numerous factors such as nutrients or inflammatory, hormonal and neuronal mediators [51,52]. ZO-1 is a scaffolding tight junction protein connecting cytoskeleton proteins and transmembrane tight junction proteins, maintaining the sealing of the intestinal barrier. In our study, we observed a significant decrease of ZO-1 expression in the hypoganglionnotic recto-sigmoid of piglets by western blot and immunohistochemistry. These results are consistent with the inverse correlation between intestinal permeability and ZO-1 expression [52], and could explain the paracellular permeability increase found in our model. Claudin 3 belongs to the claudin family, a large family of transmembrane proteins, which defines the selectivity of the paracellular permeability through homotypic and heterotypic interactions. Despite the increase in recto-sigmoid epithelial barrier permeability observed in BAC piglets, the expression of claudin 3 was increased in these animals. Similar results have been reported previously by Ueno et al. in malnourished mice exhibiting increased claudin 3 immunostaining together with increased gut permeability [53]. The association of decreased ZO-1 and increased claudin 3 expression was also described in the jejunum after bariatric surgery using Western blot techniques [54]. The third protein analyzed in this study does not belong to the TJ complex but to adherens junctions (AJ), located immediately below TJ and providing a dynamic adhesive connection between cells. E-cadherin, a transmembrane glycoprotein, is a major component of AJ. In our piglet model, e-cadherin expression increased in the hypoganglionnotic zone of the recto-sigmoid epithelium. E-cadherin expression has been shown to be modulated in several chronic intestinal inflammation

15

conditions, either down-regulated in inflammatory bowel disease [55] but also up-regulated in

5-fluoro-uracil induced mucositis in mice [56]. Together with claudin 3, increased e-cadherin

could be compensatory mechanisms to counteract the dramatic decrease in ZO-1

expression. Another possibility is that BAC-induced enteric denervation interferes with the

normal post-natal development of TJ and AJ protein expression in the epithelium. One can

imagine a natural ENS-mediated decrease in claudin-3 and e-cadherin expression with age

that is blocked by hypoganglionnosis in our model. However, such hypothesis needs further

investigations.

Another feature of our piglet BAC model is the alteration of the recto-sigmoid luminal

microbiota composition in BAC-treated piglets. For technical reasons, we were not able to

analyze microbiota composition in all animals (4 out 5 and 6 out of 7 for SHAM and BAC

piglets, respectively). Moreover, the luminal microbiota is different from the adherent one

[57]. Thus, sampling the adherent microbiota facing the hypoganglionnotic region of the

recto-sigmoid would have been also interesting. However, due to the limited length of the

treated segment, we decided to focus on various mucosal investigations and not to

investigate the adherent microbiota. These preliminary data on luminal microbiota showed

that diversity and richness were not altered by BAC treatment, but the bacterial composition

was different, as indicated by the β-diversity. Pierre et al found similar results in *Ednrb*-null

mice [58] with Chao-1 and Shannon index similar to controls at an early stage. Then,

diversity remained high in null mice and decreased in controls. The results of these two

animal studies differ with the recent HD patients' series from Neuvonen et al [59] that stated

that HD patients had an immature microbiome composition with decreased microbial

richness. This conclusion has to be waived by the fact that nearly 80% of their cohort has

had enterocolitis, 50% recurrent HAEC and thus underwent multiple courses of antibiotics

that modify microbiota composition.

In our study, three genera characterized the BAC piglet microbiota: *Bilophila, Fusobacterium*

and *Mogibacterium*. *Bilophila* belongs to the Proteobacteria phylum and has been implicated

in diseased conditions such as colitis and metabolic syndrome [60]. *Fusobacterium* belongs to the Fusobacteria phylum and is identified as a pro-inflammatory commensal bacteria [61]. Finally, *Mogibacterium*, a Firmicutes, is found in the underdeveloped piglet mucosa [62] and in the oral cavity of patients with periodontitis [63]. Taken together, these data indicate a pro-inflammatory microbiota in the recto-sigmoid lumen of BAC-treated piglets, highlighting that hypoganglionnosis can also alter intestinal microbiota development.

In conclusion we present a promising large animal model of reproducible partial denervation of the recto-sigmoid myenteric and sub-mucosal plexi. This hypoganglionnosis caused major changes of the intestinal barrier with increase of transcellular and paracellular permeabilities and profound remodeling of TJ protein expression. Although a direct effect of BAC on the epithelium cannot be firmly excluded, we are quite confident that the observed effects are due to hypoganglionnosis since no effect was observed at an earlier time-point. Alteration of the luminal microbiota towards a pro-inflammatory microbiota was also noticed in the hypoganglionnotic segment, suggesting that ENS is a major contributor to the establishment of a healthy microbiota-host interaction during the neonatal period.

Author contribution

APA and GB: designed study, performed experiments, analyzed data, wrote manuscript, JH, PB, FLG, JG, MF, GR: performed experiments, analyzed data, SH: analyzed and interpreted data, all authors reviewed and approved the manuscript.

Competing Interests

The authors declare no competing interest.

References

[1]   Kenny SE, Tam PKH, Garcia-Barcelo M. Hirschsprung's disease. Semin Pediatr Surg 2010;19:194–200. https://doi.org/10.1053/j.sempedsurg.2010.03.004.

[2]   Heanue TA, Pachnis V. Enteric nervous system development and Hirschsprung's disease: advances in genetic and stem cell studies. Nat Rev Neurosci 2007;8:466–79. https://doi.org/10.1038/nrn2137.

[3]   Austin KM. The pathogenesis of Hirschsprung's disease-associated enterocolitis. Semin Pediatr Surg 2012;21:319–27. https://doi.org/10.1053/j.sempedsurg.2012.07.006.

[4]   Moore SW, Sidler D, Zaahl MG. The ITGB2 immunomodulatory gene (CD18), enterocolitis, and Hirschsprung's disease. J Pediatr Surg 2008;43:1439–44. https://doi.org/10.1016/j.jpedsurg.2007.12.057.

[5]   Goulet O. Potential role of the intestinal microbiota in programming health and disease. Nutr Rev 2015;73 Suppl 1:32–40. https://doi.org/10.1093/nutrit/nuv039.

[6]   Neunlist M, Toumi F, Oreschkova T, Denis M, Leborgne J, Laboisse CL, et al. Human ENS regulates the intestinal epithelial barrier permeability and a tight junction-associated protein ZO-1 via VIPergic pathways. Am J Physiol Gastrointest Liver Physiol 2003;285:G1028-1036. https://doi.org/10.1152/ajpgi.00066.2003.

[7]   Toumi F, Neunlist M, Cassagnau E, Parois S, Laboisse CL, Galmiche J-P, et al. Human submucosal neurones regulate intestinal epithelial cell proliferation: evidence from a novel co-culture model. Neurogastroenterol Motil Off J Eur Gastrointest Motil Soc 2003;15:239–42.

[8]   Hayden UL, Carey HV. Neural control of intestinal ion transport and paracellular permeability is altered by nutritional status. Am J Physiol Regul Integr Comp Physiol 2000;278:R1589-1594. https://doi.org/10.1152/ajpregu.2000.278.6.R1589.

[9]   Kimm MH, Curtis GH, Hardin JA, Gall DG. Transport of bovine serum albumin across rat jejunum: role of the enteric nervous system. Am J Physiol 1994;266:G186-193. https://doi.org/10.1152/ajpgi.1994.266.2.G186.

[10]   Ward NL, Pieretti A, Dowd SE, Cox SB, Goldstein AM. Intestinal aganglionosis is associated with early and sustained disruption of the colonic microbiome. Neurogastroenterol Motil Off J Eur Gastrointest Motil Soc 2012;24:874-e400. https://doi.org/10.1111/j.1365-2982.2012.01937.x.

[11]   Roura E, Koopmans S-J, Lallès J-P, Le Huerou-Luron I, de Jager N, Schuurman T, et al. Critical review evaluating the pig as a model for human nutritional physiology. Nutr Res Rev 2016;29:60–90. https://doi.org/10.1017/S0954422416000020.

[12]   Miller ER, Ullrey DE. The pig as a model for human nutrition. Annu Rev Nutr 1987;7:361–82. https://doi.org/10.1146/annurev.nu.07.070187.002045.

[13]   Bailey M, Haverson K, Inman C, Harris C, Jones P, Corfield G, et al. The development of the mucosal immune system pre- and post-weaning: balancing regulatory and effector function. Proc Nutr Soc 2005;64:451–7.

[14]   Bustad LK, McClellan RO. Swine in biomedical research. Science 1966;152:1526–30. https://doi.org/10.1126/science.152.3728.1526.

[15]   Zhang Q, Widmer G, Tzipori S. A pig model of the human gastrointestinal tract. Gut Microbes 2013;4:193–200. https://doi.org/10.4161/gmic.23867.

[16]   Nejdfors P, Ekelund M, Jeppsson B, Weström BR. Mucosal in vitro permeability in the intestinal tract of the pig, the rat, and man: species- and region-related differences. Scand J Gastroenterol 2000;35:501–7.

[17]   Lee JE, Lee S, Sung J, Ko G. Analysis of human and animal fecal microbiota for microbial source tracking. ISME J 2011;5:362–5. https://doi.org/10.1038/ismej.2010.120.

[18]   Pang X, Hua X, Yang Q, Ding D, Che C, Cui L, et al. Inter-species transplantation of gut microbiota from human to pigs. ISME J 2007;1:156–62. https://doi.org/10.1038/ismej.2007.23.

[19]   Che C, Pang X, Hua X, Zhang B, Shen J, Zhu J, et al. Effects of human fecal flora on intestinal morphology and mucosal immunity in human flora-associated piglet. Scand J Immunol 2009;69:223–33. https://doi.org/10.1111/j.1365-3083.2008.02211.x.

[20]   Sato A, Yamamoto M, Imamura K, Kashiki Y, Kunieda T, Sakata K. Pathophysiology of aganglionic colon and anorectum: an experimental study on aganglionosis produced by a new method in the rat. J Pediatr Surg 1978;13:399–435.

[21]   Parr EJ, Sharkey KA. Multiple mechanisms contribute to myenteric plexus ablation induced by benzalkonium chloride in the guinea-pig ileum. Cell Tissue Res 1997;289:253–64.

[22]   See NA, Epstein ML, Schultz E, Pienkowski TP, Bass P. Hyperplasia of jejunal smooth muscle in the myenterically denervated rat. Cell Tissue Res 1988;253:609–17.

[23]   Wagner JP, Sullins VF, Dunn JCY. A novel in vivo model of permanent intestinal aganglionosis. J Surg Res 2014;192:27–33. https://doi.org/10.1016/j.jss.2014.06.010.

[24]   Oliveira JS, Llorach-Velludo MA, Sales-Neto VN. Megacolon in rats. Digestion 1990;45:166–71.

[25]   Yoneda A, Shima H, Nemeth L, Oue T, Puri P. Selective chemical ablation of the enteric plexus in mice. Pediatr Surg Int 2002;18:234–7. https://doi.org/10.1007/s003830100681.

[26]   Sakata K, Kunieda T, Furuta T, Sato A. Selective destruction of intestinal nervous elements by local application of benzalkonium solution in the rat. Experientia 1979;35:1611–3.

[27]   Pan WK, Zheng BJ, Gao Y, Qin H, Liu Y. Transplantation of neonatal gut neural crest progenitors reconstructs ganglionic function in benzalkonium chloride-treated homogenic rat colon. J Surg Res 2011;167:e221-230. https://doi.org/10.1016/j.jss.2011.01.016.

[28]   Laranjeira C, Sandgren K, Kessaris N, Richardson W, Potocnik A, Vanden Berghe P, et al. Glial cells in the mouse enteric nervous system can undergo neurogenesis in response to injury. J Clin Invest 2011;121:3412–24. https://doi.org/10.1172/JCI58200.

[29]   D'Errico F, Goverse G, Dai Y, Wu W, Stakenborg M, Labeeuw E, et al. Estrogen receptor β controls proliferation of enteric glia and differentiation of neurons in the myenteric plexus after damage. Proc Natl Acad Sci U S A 2018;115:5798–803. https://doi.org/10.1073/pnas.1720267115.

[30]   Arnaud AP, Rome V, Richard M, Formal M, David-Le Gall S, Boudry G. Post-natal co-development of the microbiota and gut barrier function follows different paths in the small and large intestine in piglets. FASEB J Off Publ Fed Am Soc Exp Biol 2020;34:1430–46. https://doi.org/10.1096/fj.201902514R.

[31]   Escudié F, Auer L, Bernard M, Mariadassou M, Cauquil L, Vidal K, et al. FROGS: Find, Rapidly, OTUs with Galaxy Solution. Bioinforma Oxf Engl 2018;34:1287–94. https://doi.org/10.1093/bioinformatics/btx791.

[32]   Segata N, Izard J, Waldron L, Gevers D, Miropolsky L, Garrett WS, et al. Metagenomic biomarker discovery and explanation. Genome Biol 2011;12:R60. https://doi.org/10.1186/gb-2011-12-6-r60.

[33]   Jung SY, Kim HY, Park HS, Yin XY, Chung SM, Kim HS. Standardization of A Physiologic Hypoparathyroidism Animal Model. PloS One 2016;11:e0163911. https://doi.org/10.1371/journal.pone.0163911.

[34]   Fox DA, Epstein ML, Bass P. Surfactants selectively ablate enteric neurons of the rat jejunum. J Pharmacol Exp Ther 1983;227:538–44.

[35]   Ramalho FS, Santos GC, Ramalho LN, Kajiwara JK, Zucoloto S. Myenteric neuron number after acute and chronic denervation of the proximal jejunum induced by

benzalkonium chloride. Neurosci Lett 1993;163:74–6.

[36]   Cracco C, Filogamo G. Mesenteric neurons in the adult rat are responsive to ileal treatment with benzalkonium chloride. Int J Dev Neurosci Off J Int Soc Dev Neurosci 1993;11:49–61.

[37]   Hosoda K, Hammer RE, Richardson JA, Baynash AG, Cheung JC, Giaid A, et al. Targeted and natural (piebald-lethal) mutations of endothelin-B receptor gene produce megacolon associated with spotted coat color in mice. Cell 1994;79:1267–76.

[38]   Herbarth B, Pingault V, Bondurand N, Kuhlbrodt K, Hermans-Borgmeyer I, Puliti A, et al. Mutation of the Sry-related Sox10 gene in Dominant megacolon, a mouse model for human Hirschsprung disease. Proc Natl Acad Sci U S A 1998;95:5161–5.

[39]   Brizzolara A, Torre M, Favre A, Pini Prato A, Bocciardi R, Martucciello G. Histochemical study of Dom mouse: A model for Waardenburg-Hirschsprung's phenotype. J Pediatr Surg 2004;39:1098–103.

[40]   Heinritz SN, Mosenthin R, Weiss E. Use of pigs as a potential model for research into dietary modulation of the human gut microbiota. Nutr Res Rev 2013;26:191–209. https://doi.org/10.1017/S0954422413000152.

[41]   van Ginneken C, van Meir F, Sys S, Weyns A. Stereologic description of the changing expression of constitutive nitric oxide synthase and heme oxygenase in the enteric plexuses of the pig small intestine during development. J Comp Neurol 2001;437:118–28.

[42]   Hens J, Schrödl F, Brehmer A, Adriaensen D, Neuhuber W, Scheuermann DW, et al. Mucosal projections of enteric neurons in the porcine small intestine. J Comp Neurol 2000;421:429–36.

[43]   Balemba OB, Grøndahl ML, Mbassa GK, Semuguruka WD, Hay-Smith A, Skadhauge E, et al. The organisation of the enteric nervous system in the submucous and mucous layers of the small intestine of the pig studied by VIP and neurofilament protein immunohistochemistry. J Anat 1998;192 (Pt 2):257–67.

[44]   Balemba OB, Hay-Schmidt A, Assey RJ, Kahwa CKB, Semuguruka WD, Dantzer V. An immunohistochemical study of the organization of ganglia and nerve fibres in the mucosa of the porcine intestine. Anat Histol Embryol 2002;31:237–46.

[45]   De Quelen F, Chevalier J, Rolli-Derkinderen M, Mourot J, Neunlist M, Boudry G. n-3 polyunsaturated fatty acids in the maternal diet modify the postnatal development of nervous regulation of intestinal permeability in piglets. J Physiol 2011;589:4341–52. https://doi.org/10.1113/jphysiol.2011.214056.

[46]   Blais A, Aymard P, Lacour B. Paracellular calcium transport across Caco-2 and HT29 cell monolayers. Pflugers Arch 1997;434:300–5. https://doi.org/10.1007/s004240050400.

[47]   Hällgren A, Flemström G, Nylander O. Interaction between neurokinin A, VIP, prostanoids, and enteric nerves in regulation of duodenal function. Am J Physiol 1998;275:G95-103.

[48]   Dye JF, Leach L, Clark P, Firth JA. Cyclic AMP and acidic fibroblast growth factor have opposing effects on tight and adherens junctions in microvascular endothelial cells in vitro. Microvasc Res 2001;62:94–113. https://doi.org/10.1006/mvre.2001.2333.

[49]   Bijlsma PB, Kiliaan AJ, Scholten G, Heyman M, Groot JA, Taminiau JA. Carbachol, but not forskolin, increases mucosal-to-serosal transport of intact protein in rat ileum in vitro. Am J Physiol 1996;271:G147-155. https://doi.org/10.1152/ajpgi.1996.271.1.G147.

[50]   Schmittenbecher PP, Schuster F, Heinz-Erian P, Gais P. Colonic mucosal vasoactive intestinal peptide receptors in malformations of the enteric nervous system are reduced compared with morphologically normal innervated colon. Pediatr Surg Int 2002;18:264–8. https://doi.org/10.1007/s003830100687.

[51]   Landy J, Ronde E, English N, Clark SK, Hart AL, Knight SC, et al. Tight junctions in inflammatory bowel diseases and inflammatory bowel disease associated colorectal cancer.

World J Gastroenterol 2016;22:3117–26. https://doi.org/10.3748/wjg.v22.i11.3117.

[52]   Hu CH, Xiao K, Luan ZS, Song J. Early weaning increases intestinal permeability, alters expression of cytokine and tight junction proteins, and activates mitogen-activated protein kinases in pigs. J Anim Sci 2013;91:1094–101. https://doi.org/10.2527/jas.2012-5796.

[53]   Ueno PM, Oriá RB, Maier EA, Guedes M, de Azevedo OG, Wu D, et al. Alanyl-glutamine promotes intestinal epithelial cell homeostasis in vitro and in a murine model of weanling undernutrition. Am J Physiol Gastrointest Liver Physiol 2011;301:G612-622. https://doi.org/10.1152/ajpgi.00531.2010.

[54]   Casselbrant A, Elias E, Fändriks L, Wallenius V. Expression of tight-junction proteins in human proximal small intestinal mucosa before and after Roux-en-Y gastric bypass surgery. Surg Obes Relat Dis Off J Am Soc Bariatr Surg 2015;11:45–53. https://doi.org/10.1016/j.soard.2014.05.009.

[55]   Muise AM, Walters TD, Glowacka WK, Griffiths AM, Ngan B-Y, Lan H, et al. Polymorphisms in E-cadherin (CDH1) result in a mis-localised cytoplasmic protein that is associated with Crohn's disease. Gut 2009;58:1121–7. https://doi.org/10.1136/gut.2008.175117.

[56]   Li H-L, Lu L, Wang X-S, Qin L-Y, Wang P, Qiu S-P, et al. Alteration of Gut Microbiota and Inflammatory Cytokine/Chemokine Profiles in 5-Fluorouracil Induced Intestinal Mucositis. Front Cell Infect Microbiol 2017;7:455. https://doi.org/10.3389/fcimb.2017.00455.

[57]   Sommer F, Bäckhed F. Know your neighbor: Microbiota and host epithelial cells interact locally to control intestinal function and physiology. BioEssays News Rev Mol Cell Dev Biol 2016;38:455–64. https://doi.org/10.1002/bies.201500151.

[58]   Pierre JF, Barlow-Anacker AJ, Erickson CS, Heneghan AF, Leverson GE, Dowd SE, et al. Intestinal dysbiosis and bacterial enteroinvasion in a murine model of Hirschsprung's disease. J Pediatr Surg 2014;49:1242–51. https://doi.org/10.1016/j.jpedsurg.2014.01.060.

[59]   Neuvonen MI, Korpela K, Kyrklund K, Salonen A, de Vos W, Rintala RJ, et al. Intestinal Microbiota in Hirschsprung Disease. J Pediatr Gastroenterol Nutr 2018;67:594–600. https://doi.org/10.1097/MPG.0000000000001999.

[60]   Devkota S, Wang Y, Musch MW, Leone V, Fehlner-Peach H, Nadimpalli A, et al. Dietary-fat-induced taurocholic acid promotes pathobiont expansion and colitis in Il10-/- mice. Nature 2012;487:104–8. https://doi.org/10.1038/nature11225.

[61]   Bashir A, Miskeen AY, Hazari YM, Asrafuzzaman S, Fazili KM. Fusobacterium nucleatum, inflammation, and immunity: the fire within human gut. Tumour Biol J Int Soc Oncodevelopmental Biol Med 2016;37:2805–10. https://doi.org/10.1007/s13277-015-4724-0.

[62]   Berding K, Wang M, Monaco MH, Alexander LS, Mudd AT, Chichlowski M, et al. Prebiotics and Bioactive Milk Fractions Affect Gut Development, Microbiota, and Neurotransmitter Expression in Piglets. J Pediatr Gastroenterol Nutr 2016;63:688–97. https://doi.org/10.1097/MPG.0000000000001200.

[63]   Camelo-Castillo AJ, Mira A, Pico A, Nibali L, Henderson B, Donos N, et al. Subgingival microbiota in health compared to periodontitis and the influence of smoking. Front Microbiol 2015;6:119. https://doi.org/10.3389/fmicb.2015.00119.

Figure 1: Typical examples of recto-sigmoid 21 days after BAC-treatment in piglets.

A: DAPI staining showing the overall architecture of the tissue. B: PGP9.5 immunostaining. White arrows design ganglia. Red arrows delimit the section where no ganglia were observed in the myenteric plexus.

Figure 2: Effect of BAC on recto-sigmoid ganglia number and surface area.

Number of ganglia in the myenteric (A) and outer sub-mucosal (D) plexi, average surface area of ganglia in the myenteric (B) and outer sub-mucosal (E) plexi and total surface area of ganglia in the myenteric (C) and sub-mucosal (F) plexi of SHAM (open bars, n=5) and BAC (solid bars, n=7) treated piglets. Means +/- SEM. * $P<0.05$.

Figure 3: Effect of BAC on tissue morphology.

Circular (A) and longitudinal (B) muscle layers thickness and crypt depth (C) of the ante-mesenteric side of the recto-sigmoid of SHAM (open bars, n=5) and BAC (solid bars, n=7) piglets. Means +/- SEM, * $P<0.05$.

Figure 4: Effect of BAC on epithelial barrier function.

Short-circuit current (A), conductance (B), permeability to HRP (C) and FD4 (D) of the ante-mesenteric side of the recto-sigmoid of SHAM (open bars, n=5) and BAC (solid bars, n=7) piglets. Means +/- SEM, * $P<0.05$, # $P<0.07$

Figure 5: Effect of BAC on tight and adherens junction protein expression.

Quantification of blot density (A, E, I), typical Western blot (B, F, J), typical example of immunostaining (C-D, G-H and K-L) for ZO-1, claudin 3 and e-cadherin (e-cdh), respectively of the ante-mesenteric side of the recto-sigmoid of BAC and SHAM piglets (Western blot data) or of mesenteric and ante-mesenteric sides of the recto-sigmoid in BAC piglets (immuno-staining). Means +/- SEM, n=5-7 per group. * $P<0.05$.

Figure 6: Effect of BAC on microbiota composition

PCoA of Bray-Curtis distances (A), diversity indexes (B), phyla composition (C) and LDA effect size cladrogramm (D) of BAC (n=6) and SHAM (n=4) recto-sigmoid luminal microbiota.
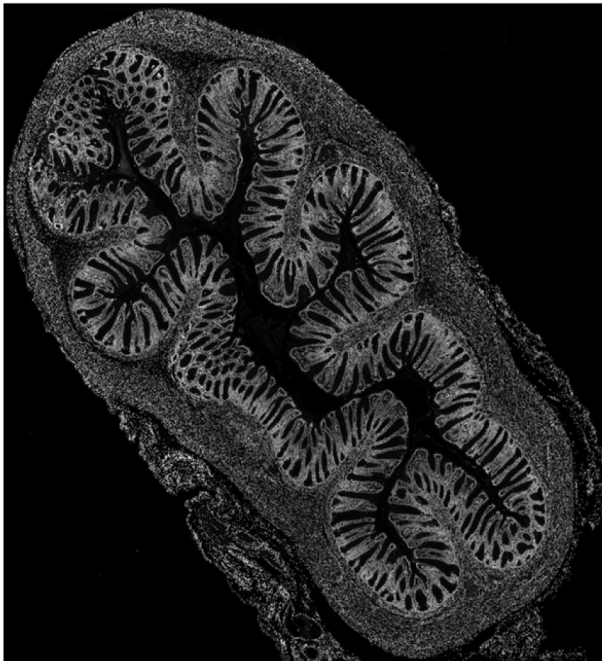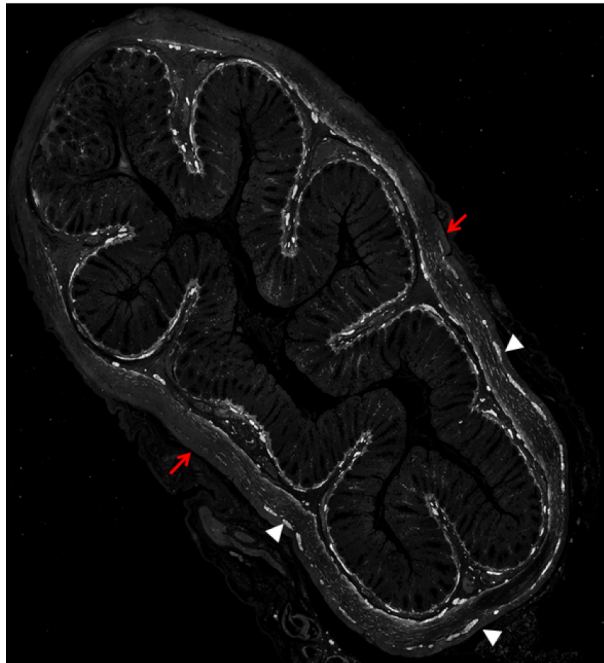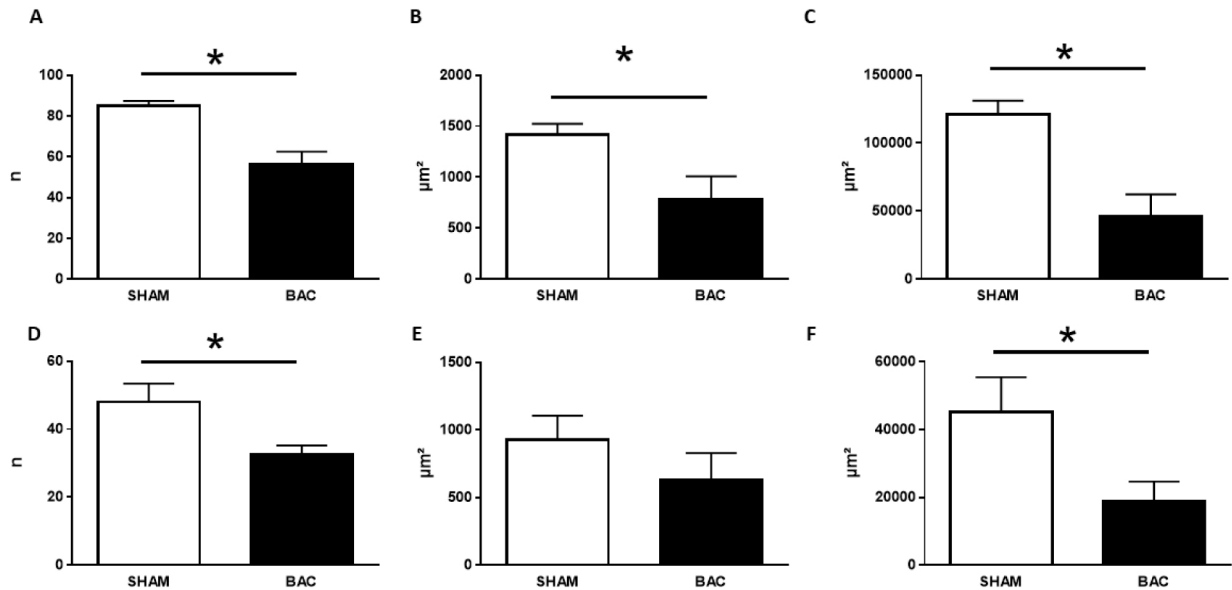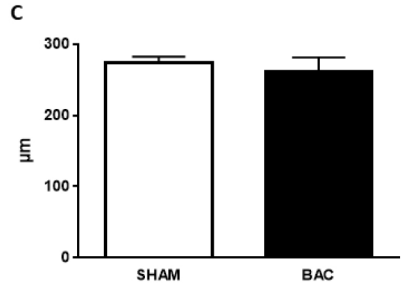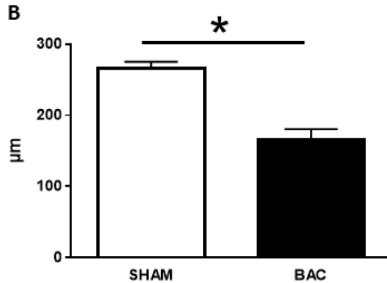
Figure 1

Figure 2

Figure 3

Figure 4

MESENTERIC SIDE   ANTE-MESENTERIC SIDE

Figure 5

Figure 6